



Research Article

Numerical Simulation of a Solar Cooling System Based on Variable-Effect NH₃-Water Absorption Chiller using TRNSYS

Abir Hmida ^a, Abdelghafour Lamrani ^b, Mamdouh El Haj Assad ^{c*}, Yashar Aryanfar ^d, Jorge Luis Garcia Alcaraz ^e

^a Applied Thermodynamics Research Laboratory, National Engineering School of Gabes, University of Gabes, Zrig Eddakhlania 6029, Gabes, Tunisia.

^b Mohamed Rougui's Lab, Mohammadia School of Engineers, University of King Mohammed V., Rabat, Morocco.

^c Department of Sustainable and Renewable Energy Engineering, University of Sharjah, Sharjah, United Arab Emirates.

^d Department of Electric Engineering and Computers Sciences, Autonomous University of Ciudad Juarez, Ciudad Juárez 32310, Chih, Mexico.

^e Department of Industrial Engineering and Manufacturing, Autonomous University of Ciudad Juarez, Ciudad Juárez 32310, Chih, Mexico.

PAPER INFO

Paper History:

Received: 09 February 2022

Revised: 18 June 2022

Accepted: 23 June 2022

Keywords:

Absorption Systems,
Solar Collectors,
Simulation,
Energy Efficiency,
TRNSYS

ABSTRACT

Around the globe, a 60 % increase in energy demand is predicted to occur by the end of the year 2030 due to the ever-increasing population and development. With a registered temperature up to 50 °C in August 2020, which is classified as one of the hottest regions in the world, the demand for cool temperatures in Gabes-Tunisia to achieve the thermal comfort of people ensuring the product storage has become more and more intense. Removing heat from buildings represents the most extensive energy consumption process. In this paper, an absorption-refrigeration system driven by solar energy is proposed. A parametric simulation model is developed based on the TRNSYS platform. A comparison between different models for global radiation calculation and experimental meteorological data was carried out. It has been proven that the Brinchambaut model seems to be the most convenient in describing the real global radiation, with an error of up to 3.16 %. An area of 22 m² of evacuated tube solar collector ensures the proper functioning of the generator and achieves a temperature up to 2 °C in the cold room.

<https://doi.org/10.30501/jree.2022.326640.1318>

1. INTRODUCTION

Despite a 3.8 % fall in worldwide energy demand due to the Covid-19 lockdown and an 8 % decline in global coal demand Global Energy and CO₂ Emissions in 2020 – Global Energy Review 2020 – Analysis - IEA, cooling and heating in buildings continue to be the leading energy consumers. With an ever-growing population, industrial development, and human life enhancement (Almutairi et al., 2022; Pan et al., 2020), with many parts of the world experiencing record-breaking temperatures, the need for cooling to ensure people's comfort and food storage is expanding significantly and has tripled since 1990 (Global Energy and CO₂ Emissions in 2020 – Global Energy Review 2020 – Analysis - IEA; Sudhakar et al., 2019). In many countries, the primary cooling source is electrical power (Asim & Kanan, 2016; Shoaib et al., 2018). According to the IEA, space cooling accounted for over 8.5 % of total final electricity consumption in 2019 and approximately 15 % of peak electricity demand on hot days (Cooling – Analysis - IEA). The majority of electrical systems rely on fossil fuels (Shoaib et al., 2018), resulting in a rise in emissions to around 1 Gt of CO₂ in 2019 and at ambient

temperature as well (Cooling – Analysis - IEA), contributing to global warming and ozone depletion concerns (Pan et al., 2020).

As a result, efforts to combat climate change must place a premium on decarbonizing energy technologies. Environmentally friendly and energy-efficient technology must be developed to mitigate the environmental impact of cooling required in the building industry while keeping costs reasonable (Gebreslassie et al., 2012; Hmida et al., 2018). Harmful emissions and fossil fuel consumption can be significantly reduced using renewable energy (Shoaib et al., 2018). Thus, solar cooling systems are a viable alternative for reducing primary energy use and are an excellent solution for today's energy challenges (Dhindsa, 2020; Li et al., 2019) and as Tiwari et al. stated, solar energy is a clean, unlimited and environmentally-friendly energy source (Tiwari et al., 2020). Solar cooling systems are of particular importance when the cooling load of a building is compared to the intensity of solar radiation. Due to the system's reliance on thermal energy for cold production, solar energy for industrial and domestic applications continues to be the greatest technology for refrigeration and air conditioning, particularly in hotter areas (Cascetta et al., 2017; Salilih et al., 2020). Two common types of solar cooling systems do exist. The first type converts sunlight directly into heat using solar thermal collectors driven

*Corresponding Author's Email: massad@sharjah.ac.ae (M. El Haj Assad)
URL: https://www.jree.ir/article_155116.html



by the solar ejector, desiccant, adsorption, or absorption systems (Salilih et al., 2020; Ullah et al., 2013). The second category involves a photovoltaic module that powers the system (Ullah et al., 2013), thermoelectric refrigeration (TEC), and PV compression refrigeration (Salilih et al., 2020). Since compression systems require high-grade energy, alternative cooling systems such as absorption cooling systems are receiving greater attention than ever (Altun & Kilic, 2020).

Solar cooling absorption systems are a reliable and cost-effective alternative to other thermally operated refrigeration cycles because they can be powered by low-grade thermal energy, have a low total cost, and enjoy a higher performance coefficient than other thermally operated refrigeration cycles (Mazzei et al., 2014; Shoaib et al., 2018). Additionally, solar absorption refrigeration systems utilize ammonia, water, and lithium bromide as environmentally-friendly refrigerants, have no global warming potential, do not contribute to ozone layer depletion, and operate at a lower temperature than other vapor compressor refrigerants (Dhindsa, 2020; Gebreslassie et al., 2012).

Numerous studies and investigations in solar thermal cooling have been conducted experimentally and theoretically, examining a variety of situations, including solar thermal collectors, and demonstrating each system's efficiency and technical viability (Li et al., 2019; Lugo et al., 2019). (Kalogirou et al., 2016) conducted an exergy analysis of a solar cooling system using Flat Plate Collectors (FPCs). Zambolin and Del Col (Zambolin & Col, 2012) examined the same system using Evacuated Tubular Collectors (ETCs), and (Li et al., 2013) studied also the same system using Compound Parabolic Concentrating collectors (CPCs). Altun and Kilic concluded through TRNSYS simulation and the use of evacuated tube solar collectors (ETC) instead of flat plate collectors (FPC), a decrease in auxiliary energy consumption and an increase in the useful energy can be gained from collectors. (Altun & Kilic, 2020).

(Figaj et al., 2021) investigated a solar dish-concentrating system with thermal collectors experimentally and numerically using a dynamic simulation of solar cooling installation. The TRNSYS program was used to perform a computer simulation of the dynamic operation of the solar heating and cooling system. The goal of this study was to determine the amount of heat formed by sorption chillers that are used for heating and cooling. Numerous configurations, locations, and periods were studied to determine the energy and economic performance of the system.

Jalalizadeh et al. researched "Building Integrated Photovoltaic Thermal Collector (BIPVT)", a technology to simultaneously generate heat and electricity for the building. They concluded that integration of PVT with the building increased the Space Cooling (SC) load by 5 % and decreased the space heating (SH) load by 3 % (Jalalizadeh et al., 2021).

Tashtoush et al. also developed a simulation program using TRNSYS-EES software to design the solar collector system components and evaluate the performance of solar ejector cooling systems. To produce 7 kW for the cooling system, an evacuated tube solar collector was chosen with an area of 60-70 m² and a solar fraction of 0.52-0.542 (Tashtoush et al., 2015). Space cooling has been a focus of many researchers using solar energy for air conditioning systems (Rahman et al., 2019), geothermal energy for powering single-effect water/lithium bromide absorption chiller (El Haj Assad et al.,

2021), and solar vapor compression refrigeration cycle (Aryanfar et al., 2022).

Numerous experimental research studies on solar thermal technologies have evaluated and designed them. Nonetheless, numerical simulation was used to optimize the system as several scenarios might be examined due to its cost. According to (Lugo et al., 2019), the creation of simulation software enables the identification of the behavior of various variables under various operating situations.

This paper aims to develop a model to determine the feasibility of a solar refrigeration system for a low-temperature room with a cooling capacity of 11 kW using an evacuated solar collector (ETC). The system maintains a constant temperature of 2 °C in the cold room. To predict the performance of the cooling thermally driven system for various climatic and seasonal changes in the year, a configuration model based on TRNSYS (Transient Simulation Program) is constructed and simulated. The components and connections from the standard TRNSYS library are used. The performance of the ETC under the climatic conditions of Gabes, Tunisia (33°53'N, 10°6'E) has been evaluated. The optimal collector tilt for the ETC collector was determined to be around 30°-45° (ETC), and other effects of operating parameters were evaluated and presented in the paper.

2. SYSTEM DESCRIPTION

Absorption refrigeration machines are the most used thermally driven cooling systems (Asim et al., 2016). The most used combination of fluids for low-temperature applications in absorption systems is ammonia-water (NH₃-H₂O). The absorbent (H₂O) on the low-pressure side absorbs the evaporating refrigerant (NH₃). An 8-kW solar-powered absorption system provides the cooling energy required for a cold room under different weather conditions in the region of Gabes. The cycling fluid in the system is the NH₃-H₂O. Figure 1 represents the schematic view of the model where the absorption system is the main system of the model, and it is interconnected with three subsystems: the first is the solar subsystem that consists of solar collectors and the storage tank where the ETC receives solar irradiation and is converted into thermal heat energy, which can be used to supply heat for the water tank. The second is the hot fluid subsystem, where the storage tank supplies the absorption chiller with hot water to heat the generator. The third is the load subsystem connecting the absorption chiller to the cold room (Altun & Kilic, 2020).

Low-pressure NH₃ vapor from the evaporator is dissolved in H₂O in the absorber (10) under an intermediate temperature up to 45 °C. Then, using an ordinary liquid pump (1), the resulting solution is pumped to high pressure (2, 3). The additional heat provided by the solar collector separates the NH₃ from the solution in the generator (120 °C) and then, directs it to the condenser (45 °C) (7). In this way, the NH₃ vapor is thermally compressed. Liquified refrigerant getting out from the condenser can then be expanded from this high-pressure zone (around 20 bars) (8) to the low-pressure evaporator (around 4 bars) (9). The energy required for refrigerant evaporation is extracted from the environment to be cooled. The refrigerant is then directed to the absorber (10) (Hmida et al., 2018).

On the other hand, the weak solution (with a low percentage of ammonia) is returned to the absorber (4) through a heat exchanger to recover the heat (5).

This study concentrates on the first subsystem. The thermodynamic study of the absorption chiller, as well as the cold room design, was conducted in previous studies (Hmida et al., 2017, Hmida et al., 2018, Hmida et al., 2019).

3. Modeling in TRNSYS

The model is implemented into the TRNSYS software environment, as presented in Figure 2. TRNSYS (Transient System Simulation) is an application used to model and simulate the behavior and performance of systems in a transient manner. The first step in TRNSYS simulation is identifying the individual components that better describe the

performance of the whole system (Altun & Kilic, 2020; Tiwari et al., 2020).

The TRNSYS solver performs several iterations until the inputs to all of the “Types” remain stable at each time step of the simulation.

The components used in the TRNSYS model are explained below. In order to achieve greater efficiency, the tube collectors (Type 538) evacuated from the “Tess library” were selected for the system, and then the collector circulating pump was chosen as Type 3b. An auxiliary heater (Type 4a) was used to supply hot water when solar irradiation becomes insufficient, and typical meteorological year (Type 109-TMY2) data of the region of Gabes were used from the Meteororm database of the TRNSYS library.

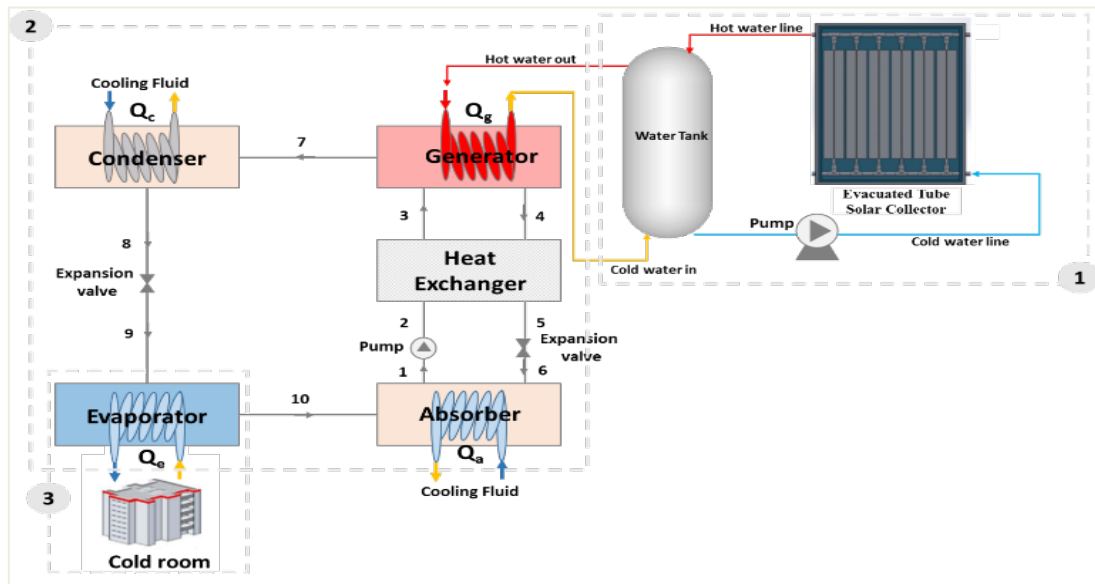


Figure 1. The schematic diagram of the solar absorption machine

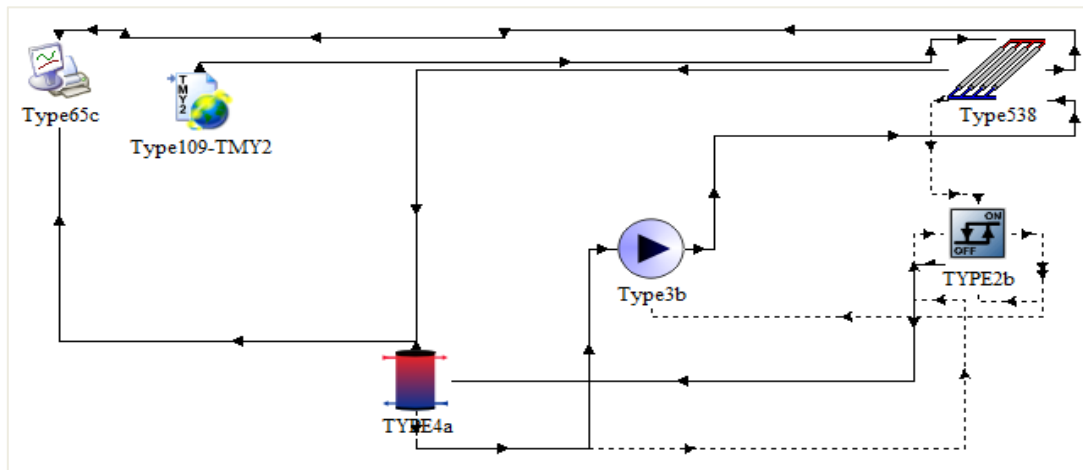


Figure 2. The solar installation with TRNSYS

4. SOLAR COLLECTOR DESIGN

4.1. Determination of the surface

Knowing that the helpful power of the solar collector depends on its surface and the local-global radiation, the needed area of the solar collector is determined using Eq. (1) to provide heat for the generator (Dezfouli et al., 2022).

$$A_c = \frac{P_u}{G \times \beta - G \times K \times (T_{fm} - T_c)} \quad (1)$$

$$P_u = 1.1 \times Q_g \quad (2)$$

where:

P_u : Useful power (kW)

Q_g : Heat absorbed by the generator (kW)

K : Heat loss coefficient (between 1.5 and 3 W/m² °C)

β : Optical coefficient for evacuated tube collector (between 0.5 and 0.8)

G : Global radiation (W/m²).

The global radiation is extracted from the climatic information of the study site. The absence of meteorological measuring stations requires establishing computational models based on empirical methods to estimate solar flux on a local scale. These models can only be applicable after comparing and validating the experimental data during all the year's seasons.

4.2. Global radiation

4.2.1. Capderou model

The well-known Capderou model was proposed to calculate the direct and diffuse radiation received on a plane (Hamed et al., 2014). On the horizontal plane, the global radiation was given as the direct radiation and the diffuse radiation sum:

$$G_h = I_h + D_h \quad (3)$$

The following equations, respectively, give direct light-sky radiation and diffuse radiation on a horizontal plane:

$$I_h = C\alpha \sin(h) \exp\left(-FTL\left(0,9 + \frac{9,4}{0,89^2} \sin(h)\right)^{-1}\right) \quad (4)$$

$$D_h = C \exp\left(-1 + 1,06 \log(\sin(h)) + a - \sqrt{a^2 + b^2}\right) \quad (5)$$

4.2.2. Euftrat model

Euftrat proposed other equations for the calculation of direct (I_i), diffuse (D_i), and global radiation (G_i) received on an inclined plane (Hamed et al., 2014). It can be obtained as:

$$I_i = C\alpha \exp\left(-\frac{AM \times FTL}{0,9 AM + 9,4}\right) \quad (6)$$

$$G_i = \alpha(1270 - 56 FTL)(\sin(h)) \left(\frac{FTL+36}{33}\right) \quad (7)$$

$$D_i = G_i - I_i \sin(h) \quad (8)$$

where:

C: Solar constant (1367 W / m²)

FTL: Linke's trouble factor

AM: Atmospheric mass

h: Height of the sun

α : Correction of the distance between earth and sun.

4.2.3. Perrin Brinchambaut model

Perrin Brinchambaut proposed the following equations for the calculation of direct (I_i), diffuse (D_i), and global radiations (G_i) received on an inclined plane as follows (Hamed et al., 2014):

$$D_i = A' \cos(\theta) \exp\left(-\frac{1}{B' \sin(h+2)}\right) \quad (9)$$

$$I_i = \left(\frac{1 + \cos(\beta)}{2}\right) D_h + \left(\frac{1 - \cos(\beta)}{2}\right) \rho G_h \quad (10)$$

The direct radiation I_h , global radiation G_h , and the albedo ρ for a horizontal plane are respectively expressed as follows:

$$I_h = A'' (\sin(h))^{0,4} \quad (11)$$

$$G_h = A''' (\sin(h))^{B''} \quad (12)$$

$$\rho = \begin{cases} = 0.9 \text{ to } 0.8 \text{ snow} \\ = 0.8 \text{ to } 0.4 \text{ Clair ground} \\ = 0.4 \text{ to } 0.2 \text{ greeneries} \end{cases} \quad (13)$$

where A' , A'' , A''' , B' , and B'' are constants depending on the state of the atmosphere given in Table 1.

Table 1. Values of constants according to the nature of the sky

Nature of the sky	A' (W/m ²)	B'	A''' (W/m ²)	A'''' (W/m ²)	B''
Major blue	1300	6	87	1150	1.15
Light blue	1230	4	125	1080	1.22
Milky blue	1200	2.5	187	990	1.25

To assess the accuracy of these correlations, two statistical tests were used: the relative deviation (or error) (ER) and the average relative deviation (ERM). Low values of ER and ERM are desirable; they are calculated by the following relationships (Hamed et al., 2014):

$$ER(\%) = 100 \times \left(\frac{\text{Experimental.Value} - \text{Theoretical.Value}}{\text{Experimental.Value}} \right) \quad (14)$$

$$ERM(\%) = \left(100 \times \sum_k^n \left| \frac{\text{Experimental.Value}_k - \text{Theoretical.Value}_k}{\text{Experimental.Value}_k} \right| \right) / n \quad (15)$$

5. RESULTS AND DISCUSSION

5.1. Site study

This study was elaborated to produce cold for 109 m³ room to preserve food (Hmida et al., 2019). The refrigeration system was driven by an absorption machine and installed in Gabes, a southern region of Tunisia (33°53'N, 10°6'E) with high solar potential and a long insolation period, particularly in June, July, and August months. In this period, refrigeration reaches its peak demand. Figure 3 exhibits the insolation data of the region of Gabes for twelve months based on the data provided by Meteonorm software. As seen, the summer season (June, July, and August) has the longest months with an average of 12 hours of sunshine and average radiation of 215kWh/m², as depicted in Figure 4, reaching an average temperature of 35 °C in July (Figure 5).

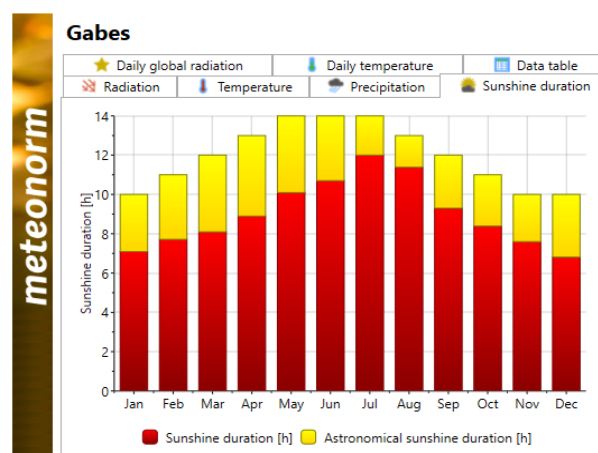


Figure 3. Sunshine period in the region of Gabes by Meteonorm 8

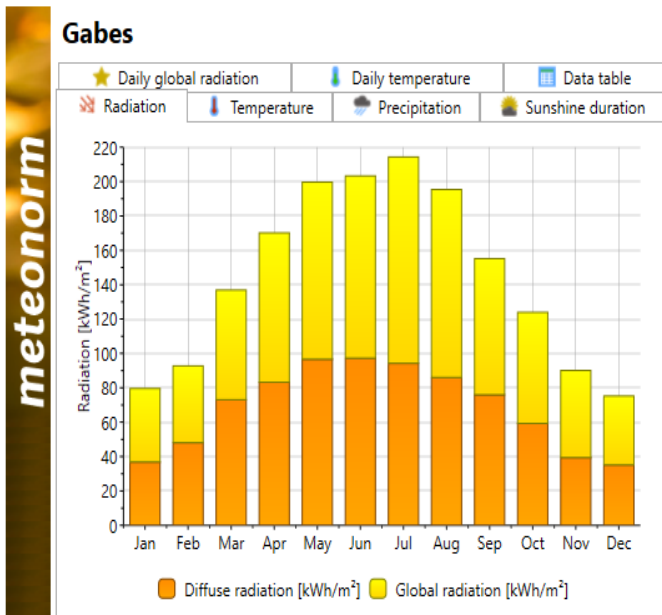


Figure 4. The region of Gabe's radiation by Meteonorm 8

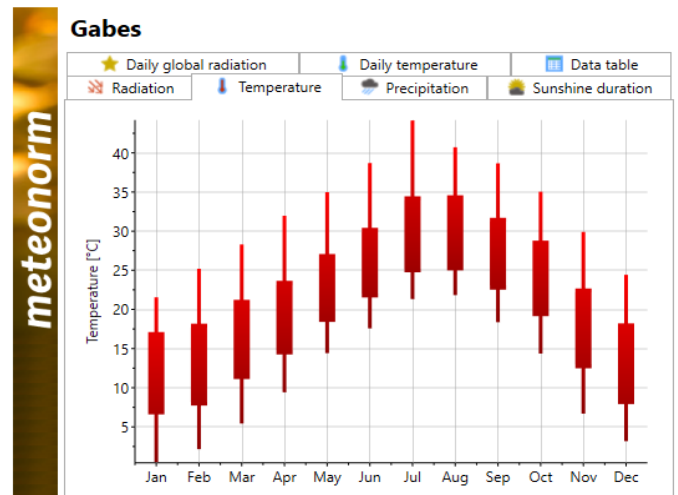


Figure 5. The average temperature of the region of Gabes by Meteonorm 8

Figure 6 shows the flowchart used in the calculation for the proposed solar/cooling system.

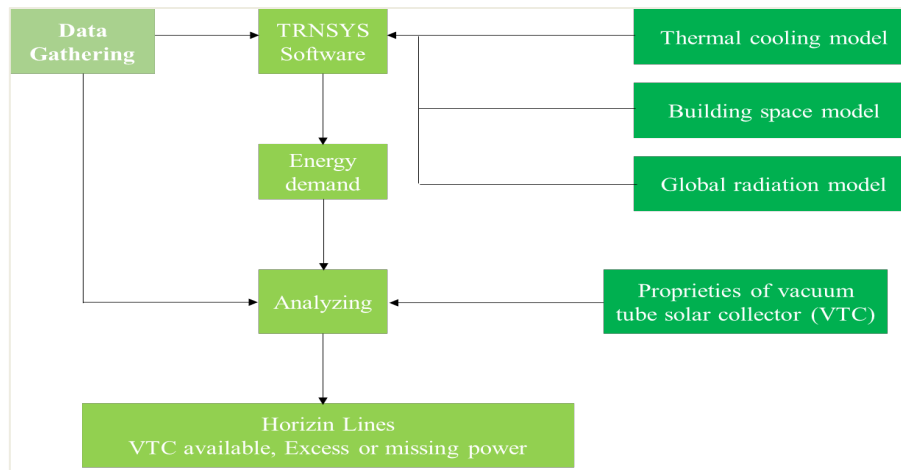


Figure 6. The flowchart of the study

The heat provided to the generator of the absorption machine is related to the ETC surface, which depends on the available global radiation. A comparison between the presented models for global radiation calculation (Eqs. 3-13) and the data provided by the National Institute of Meteorology in Tunisia (INM) was conducted.

Even though the experimental results of the global radiation for the year 2020 were not stable, as shown in Figure 7, the Brinchambaut model seems to be the most convenient in describing the real global radiation with an error of up to 3.16 % compared to 17.4 % and 20 % for the Euftrat and Capderou models, respectively.

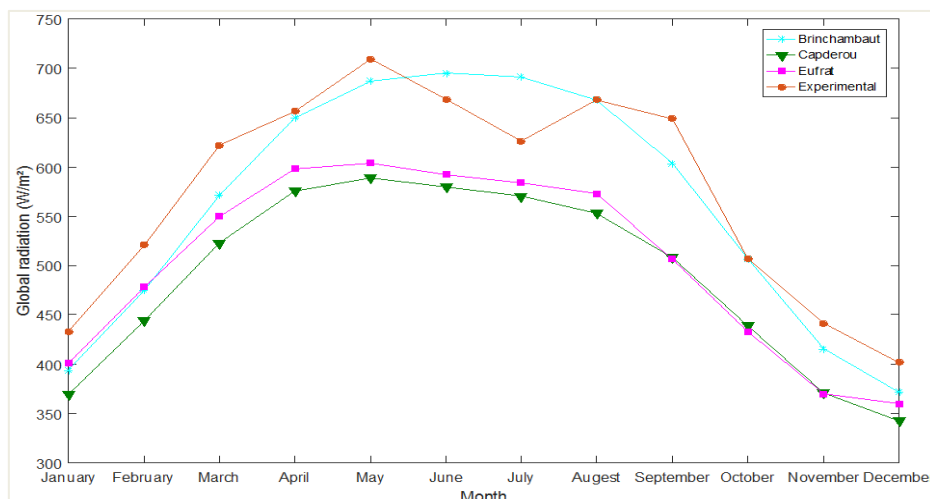


Figure 7. Comparison between the numerical models of the global radiation determination and the experimental data of the INM

5.2. TRNSYS simulation of the solar installation

The global radiation of the region of Gabes has allowed running the TRNSYS simulation. The system was simulated during the period of refrigeration need, that is, between the first of March (hour number 1416) and the last day of October (hour number 6421). As presented in Table 2, the technical characteristics of the solar system were chosen as follows: water as a heat transfer fluid (HTF) with a flow rate of 117 kg/h, the solar collector area is 21 m², producing 11 kW useful power and an average temperature on the surface up to 130 °C.

The temperature fluctuation presented in Figure 8 was due to the variation of the global radiation measured on the surface of the ETC, as presented in Figure 9. oriented to the South with a tilt equal to 45°, and 3 m²/collector as a solar collector area.

Table 2. Technical characteristics of the solar collector

VTC Parameters	
Collector area (m ²)	3
Number of solar collectors in series	7
HTF Flowrate (kg/h.m ²)	117
Efficiency slope (kJ/hr.m ² .°K)	15

In order to validate the simulation results using TRNSYS, the needed surface area using solar collector characteristics available in the market was calculated. As shown in Table 3, the needed surface area for VITSOL 200T, THERMOMAX HP100/200, and THERMOMAX DF100 is between 21 m² and 22 m², which is the surface found with TRNSYS simulation with a relative error up 2.8 %.

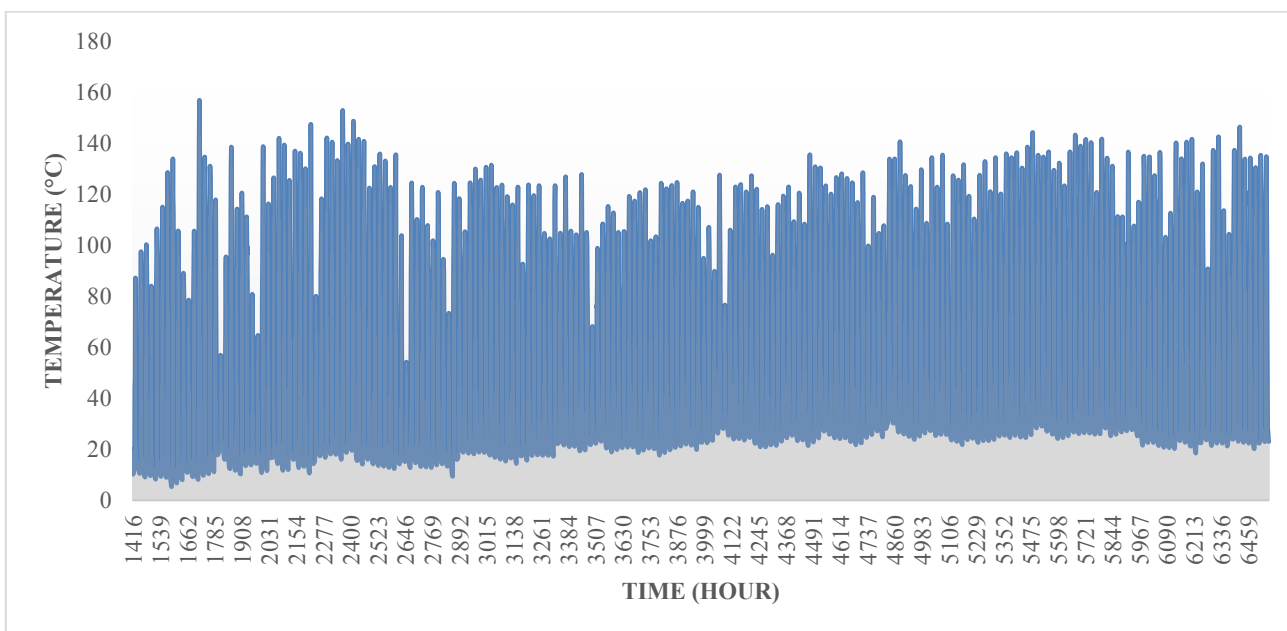


Figure 8. Hourly Temperature variation registered on the surface of the VTC

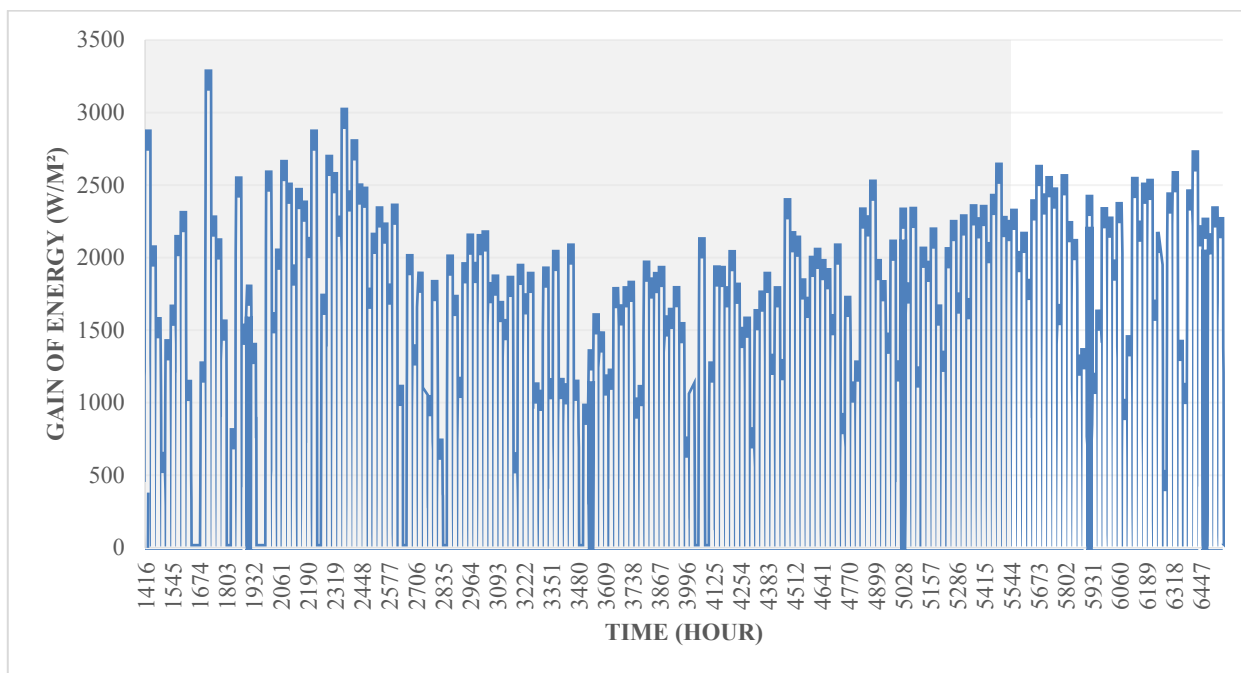


Figure 9. Global radiation fluctuation on the surface of the ETC

Table 3. Collector area and number

Collector type	Availability (m ²)	K	β	S (m ²)	N
Vitsol 200T	1,26	1,522	0.785	21.47	17
	1,51	1.443	0.801	20.59	14
	3,03	1.103	0.801	19.3	7
Thermomax HP100	3	1	0.739	20.85	7
Thermomax HP200	2	1.36	0.761	21.62	11
	3	1.36	0.761	21.62	7
Thermomax DF100	2	1.45	0.773	21.59	11
	3	1.45	0.773	21.59	7

6. CONCLUSIONS

Due to environmental problems, this study attempted to find a solution for better food storage using an available and renewable heat source. Since a good solar potential characterized the South of Tunisia, solar energy was chosen as the heat generator for the absorption machine. A simulation using TRNSYS software of a solar-based single-effect NH₃-H₂O absorption refrigeration system in a low-temperature room having a cooling capacity of 11 kW was carried out. The cold room temperature was kept at 2 °C. The weather data of the region of Gabes at latitude 33.53 N and longitude 10.6 E, collected in the year 2020, were used in the simulation.

Solar collector type, area, storage tank, and the flow rate through the cycle were investigated.

The performance of the solar collector was assessed to meet the desired outlet temperature adequate to run 11 kW cooling cycle to meet the cooling load demand. The energy requirements of 11 kW cooling system are best met with an evacuated tube solar collector having an area of 21 m² and a flow rate of 117 kg/h to provide heat for the generator in the refrigeration system.

The simulation result demonstrated that the temperature on the collector surface varied between 120 °C and 170 °C due to the global radiation fluctuation at the peak solar radiation in July. The required area of the ETC was found to be 21 m². This number can be reduced when considering the solar radiation of the summer months. The application of the sun as a heat source makes such systems economically alternative.

Other studies can follow this research by designing more environmentally-friendly buildings that meet the standards. With harmless cooling and heating load, those buildings tend to grant people comfort. In this context, simulations for air conditioning and heating systems applied to green buildings are established.

7. ACKNOWLEDGEMENT

This work was supported by the Applied Thermodynamics Research Laboratory (LR 18ES33), the University of Gabes, Tunisia. The authors would like to express their acknowledgment to the Ministry of Higher Education and Scientific Research of Tunisia.

NOMENCLATURE

AM	Atmospheric mass
C	Solar constant
CPCs	Parabolic concentrating collectors

D	Diffuse radiation (W/m ²)
ETCs	Evacuated tubular collectors
FPCs	Flat plate collectors
FTL	Linke's trouble factor
G	Global radiation (W/m ²)
GtCO ₂	Gigaton of carbon diode
h	Height of the sun
HWST	Hot water storage tanks
I	Direct radiation (W/m ²)
K	Heat loss coefficient (W/m ² °C)
NH ₃	Ammonia
P _u	Useful power (W)
PV	Photovoltaic panel
Q _g	Heat absorbed by the generator (W)
SAC	Solar adsorption cooling system
TRNSYS	Transient System Simulation TOOL
VTC	Vacuum Tube Collector
Greek letters	
α	Correction of the distance earth-sun
β	Optical coefficient for evacuated tube collector
ρ	The albedo
Subscripts	
h	Horizontal plane
i	Inclined plane

REFERENCES

- Almutairi, K., Alhuyi, M., & Salem, M. (2022). A review on applications of solar energy for preheating in power plants. *Alexandria Engineering Journal*, 61(7), 5283-5294. <https://doi.org/10.1016/j.aej.2021.10.045>
- Altun, A.F., & Kilic, M. (2020). Economic feasibility analysis with the parametric dynamic simulation of a single effect solar absorption cooling system for various climatic regions in Turkey. *Renewable Energy*, 152, 75-93. <https://doi.org/10.1016/j.renene.2020.01.055>
- Aryanfar, Y., Assad, M.E.H., Khosravi, A., Atiqure, R.S.M., Sharma, S., Alcaraz, J.L.G., & Alayi, R. (2022). Energy, exergy and economic analysis of combined solar ORC-VCC power plant. *International Journal of Low-Carbon Technologies*, 17, 196-205. <https://doi.org/10.1093/ijlct/ctab099>
- Asim, M., & Kanan, S. (2016). TRNSYS simulation of a solar cooling system for the hot climate of Pakistan. *Energy Procedia*, 91, 702-706. <https://doi.org/10.1016/j.egypro.2016.06.233>
- Cascetta, F., Lorenzo, R. Di, Nardini, S., & Cirillo, L. (2017). A TRNSYS simulation of a solar-driven air refrigerating system for a low-temperature room of an agro-industry site in the Southern of Italy. *Energy Procedia*, 126, 329-336. <https://doi.org/10.1016/j.egypro.2017.08.259>
- Cooling - Analysis - IEA*. Retrieved February 3, 2022, from <https://www.iea.org/reports/cooling>
- Dezfouli, M.M.S., Sopian, K., & Kadir, K. (2022). Energy and performance analysis of solar solid desiccant cooling systems for energy efficient buildings in tropical regions. *Energy Conversion and Management: X*, 14(November 2021), 100186. <https://doi.org/10.1016/j.ecmx.2022.100186>

8. Dhindsa, G.S. (2020). Review on performance enhancement of solar absorption refrigeration system using various designs and phase change materials. *Materials Today: Proceedings*, 37, 3332-3337. <https://doi.org/10.1016/j.matpr.2020.09.125>
9. El Haj Assad, M., Sadeghzadeh, M., Ahmadi, M.H., Al-Shabi, M., Albawab, M., Anvari-Moghaddam, A., & Bani Hani, E. (2021). Space cooling using geothermal single-effect water/lithium bromide absorption chiller. *Energy Science and Engineering*, 9(10), 1747-1760. <https://doi.org/10.1002/ese3.946>
10. Figaj, R., Zo, M., & Coil, F. (2021). Experimental and numerical analysis of hybrid solar heating and cooling system for a residential user. *Renewable Energy*, 172, 955-967. <https://doi.org/10.1016/j.renene.2021.03.091>
11. Gebreslassie, B.H., Groll, E.A., & Garimella, S.V. (2012). Multi-objective optimization of sustainable single-effect water/Lithium Bromide absorption cycle. *Renewable Energy*, 46, 100-110. <https://doi.org/10.1016/j.renene.2012.03.023>
12. *Global energy and CO₂ emissions in 2020 – Global energy review 2020 – Analysis – IEA*. (2022). Retrieved February 3, 2022, from <https://www.iea.org/reports/global-energy-review-2020/global-energy-and-co2-emissions-in-2020>
13. Hamed, M., Fellah, A. & Ben Brahim, A. (2014). Parametric sensitivity studies on the performance of a flat plate solar collector in transient behavior. *Energy Conversion and Management*, 78, 938-947. <https://doi.org/10.1016/j.enconman.2013.09.044>
14. Hmida, A., Chekir, N., & Ben Brahim, A. (2017). Solar absorption refrigerator. *International Conference on Green Energy and Conversion Systems, GECS 2017*, IEEE, Hammamet, Tunisia. <https://doi.org/10.1109/GECS.2017.8066193>
15. Hmida, A., Chekir, N., & Ben Brahim, A. (2018). Performance of an absorption refrigerator using a solar thermal collector. *International Journal of Energy and Power Engineering*, 12(10), 787-792. <https://doi.org/10.5281/zenodo.1475032>
16. Hmida, A., Chekir, N., Laafer, A., El Amine Slimani, M. & Ben Brahim, A. (2019). Modeling of cold room driven by an absorption refrigerator in the south of Tunisia: A detailed energy and thermodynamic analysis. *Journal of Cleaner Production*, 211, 1239-1249. <https://doi.org/10.1016/j.jclepro.2018.11.219>
17. Jalalizadeh, M., Fayaz, R., Delfani, S., & Jafari, H. (2021). Dynamic simulation of a trigeneration system using an absorption cooling system and building integrated photovoltaic thermal solar collectors. *Journal of Building Engineering*, 43(March), 102482. <https://doi.org/10.1016/j.jobe.2021.102482>
18. Kalogirou, S.A., Karellas, S., Braimakis, K., & Stanciu, C. (2016). Exergy analysis of solar thermal collectors and processes. *Progress in Energy and Combustion Science*, 56, 106-137. <https://doi.org/10.1016/j.peccs.2016.05.002>
19. Li, X., Dai, Y.J., Li, Y., & Wang, R.Z. (2013). Comparative study on two novel intermediate temperature CPC solar collectors with the U-shape evacuated tubular absorber. *Solar Energy*, 93, 220-234. <https://doi.org/10.1016/j.solener.2013.04.002>
20. Li, X., Lin, A., Young, C., Dai, Y., & Wang, C. (2019). Energetic and economic evaluation of hybrid solar energy systems in a residential net-zero energy building. *Applied Energy*, 254(May), 113709. <https://doi.org/10.1016/j.apenergy.2019.113709>
21. Lugo, S., Garcia-Valladares, O., Best, R., Hernández, J., & Hernández, F. (2019). Numerical simulation and experimental validation of an evacuated solar collector heating system with gas boiler backup for industrial process heating in warm climates. *Renewable Energy*, 139, 1120-1132. <https://doi.org/10.1016/j.renene.2019.02.136>
22. Mazzei, M.S., Mussati, M.C., & Mussati, S.F. (2014). NLP model-based optimal design of LiBr-H₂O absorption refrigeration systems. *International Journal of Refrigeration*, 38(1), 58-70. <https://doi.org/10.1016/j.ijrefrig.2013.10.012>
23. Pan, Q., Peng, J., & Wang, R. (2020). Application analysis of adsorption refrigeration system for solar and data center waste heat utilization. *Energy Conversion and Management*, 228, 113564. <https://doi.org/10.1016/j.enconman.2020.113564>
24. Rahman, S., Issa, S., Said, Z., El Haj Assad, M., Zadeh, R., & Barani, Y. (2019). Performance enhancement of a solar powered air conditioning system using passive techniques and SWCNT /R-407c nano refrigerant. *Case Studies in Thermal Engineering*, 16., 100565 <https://doi.org/10.1016/j.csite.2019.100565>
25. Salilih, E.M., Birhane, Y.T., & Abu-hamdeh, N.H. (2020). Performance prediction of a solar refrigeration system under various operating pressure of evaporator and condenser. *Solar Energy*, 209(March), 485-492. <https://doi.org/10.1016/j.solener.2020.09.033>
26. Shoaib, M., Khan, A., Waheed, A., Talha, T., Wajahat, M., & Sarfraz, F. (2018). Configuration based modeling and performance analysis of single effect solar absorption cooling system in TRNSYS. *Energy Conversion and Management*, 157(September 2017), 351–63. <https://doi.org/10.1016/j.enconman.2017.12.024>
27. Sudhakar, K., Jenkins, M.S., Mangal, S., & Priya, S.S. (2019). Modelling of a solar desiccant cooling system using a TRNSYS-MATLAB co-simulator: A review. *Journal of Building Engineering*, 24(February), 100749. <https://doi.org/10.1016/j.jobe.2019.100749>
28. Tashtoush, B., Alshare, A., & Al-rifai, S. (2015). Hourly dynamic simulation of solar ejector cooling system using TRNSYS for Jordanian climate. *Energy Conversion and Management*, 100, 288-299. <https://doi.org/10.1016/j.enconman.2015.05.010>
29. Tiwari, A.K., Gupta, S., Joshi, A.K., Raval, F., & Sojitra, M. (2020). TRNSYS simulation of flat plate solar collector based water heating system in Indian climatic condition. *Materials Today: Proceedings*, 46, 5360-5365. <https://doi.org/10.1016/j.matpr.2020.08.794>
30. Ullah, K.R., Saidur, R., Ping, H.W., Akikur, R.K., & Shuvo, N.H. (2013). A review of solar thermal refrigeration and cooling methods. *Renewable and Sustainable Energy Reviews*, 24, 499-513. <https://doi.org/10.1016/j.rser.2013.03.024>
31. Zambolin, E. and Del Col, D. (2012). An improved procedure for the experimental characterization of optical efficiency in evacuated tube solar collectors. *Renewable Energy*, 43, 37-46. <https://doi.org/10.1016/j.renene.2011.11.011>